Theoretical studies of gamma-ray binaries as powerful galactic accelerators

Valenti Bosch-Ramon

Universitat de Barcelona, ICCUB, IEEC

PASTO - Particle Acceleration in aSTrophysical Objects

September 6th, 2022

Outline

Outline

High-mass gamma-ray binaries (HMGB)

- **The phenomenological term *gamma-ray binary* was mostly assign to high-mass star+CO and a gamma-ray dominated SED (without the star).**
- **HMGB are among the most powerful galactic sources, with $L \sim 10^{36}$ (MeV), 10^{34-37} (GeV) and 10^{32-35} erg s^{-1} (TeV), reaching ~ 100 TeV.**
- **The great majority of the known HMGB are VHE emitters; we focus on X- and γ-rays, although radio is important for middle–large scales.**

(Some reviews: Mirabel 2006; Romero 2009; B-R & Khangulyan 2009; Dubus 2015; Paredes & Bordas 2019; Chernyakova & Malyshev 2020...)

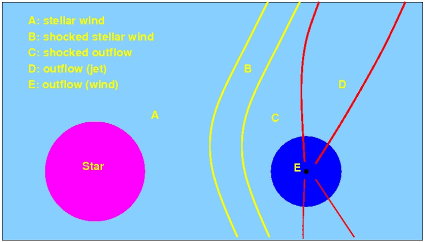

Main elements of a HMGB.

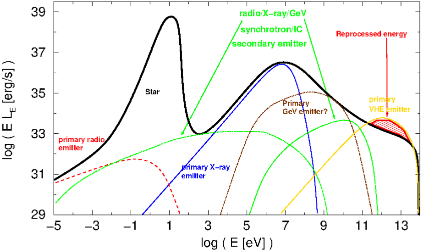

Typical SED of a HMGB.

High-mass gamma-ray binaries (HMGB)

- **The phenomenological term *gamma-ray binary* was mostly assign to high-mass star+CO and a gamma-ray dominated SED (without the star).**
- **HMGB are among the most powerful galactic sources, with $L \sim 10^{36}$ (MeV), 10^{34-37} (GeV) and 10^{32-35} erg s^{-1} (TeV), reaching ~ 100 TeV.**
- **The great majority of the known HMGB are VHE emitters; we focus on X- and γ-rays, although radio is important for middle–large scales.**

(Some reviews: Mirabel 2006; Romero 2009; B-R & Khangulyan 2009; Dubus 2015; Paredes & Bordas 2019; Chernyakova & Malyshev 2020...)

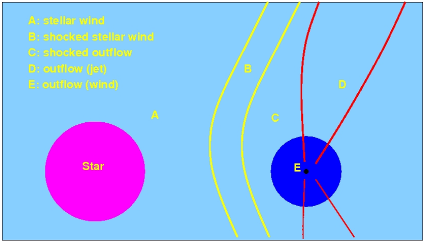

Main elements of a HMGB.

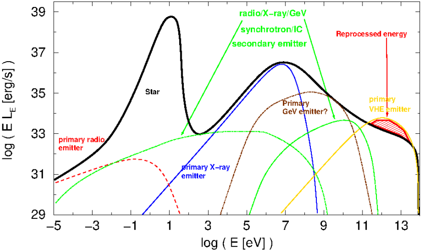

Typical SED of a HMGB.

High-mass gamma-ray binaries (HMGB)

- **The phenomenological term *gamma-ray binary* was mostly assign to high-mass star+CO and a gamma-ray dominated SED (without the star).**
- **HMGB are among the most powerful galactic sources, with $L \sim 10^{36}$ (MeV), 10^{34-37} (GeV) and 10^{32-35} erg s^{-1} (TeV), reaching ~ 100 TeV.**
- **The great majority of the known HMGB are VHE emitters; we focus on X- and γ-rays, although radio is important for middle–large scales.**

(Some reviews: Mirabel 2006; Romero 2009; B-R & Khangulyan 2009; Dubus 2015; Paredes & Bordas 2019; Chernyakova & Malyshev 2020...)

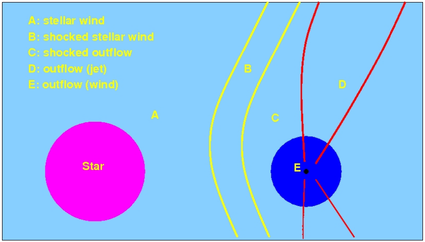

Main elements of a HMGB.

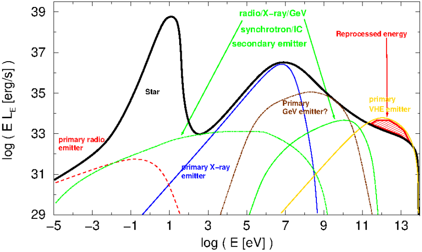

Typical SED of a HMGB.

Non-accreting vs accreting HMGB

- **A non-accreting HMGB consists of a young pulsar plus an OB star whose winds interact in the ejector regime (mostly).**
- A HMMQ consists of a CO plus an OB star in which the wind is accreted and jets form, which interact with the wind.
- In both cases, outflows interacting along the orbit are complex and emit radio, X- and γ-rays, likely through synchrotron and IC, plus $\gamma\gamma$...

(e.g., B-R, Khangulyan, Aharonian, Barkov, Perucho + ...;

Bogovalov, + ...; Romero, + ...; Dubus, Lamberts, Cerutti + ...;

Sierpowska-Bartosik, Torres, Papitto + ...; Bednarek, + ...;

Huber, Kissmann, Reimer, + ...; Yoon, Heinz, Zdziarski + ...;

Chernyakova, Neronov, + ...; Takata, Kong, Cheng, + ...; etc.)

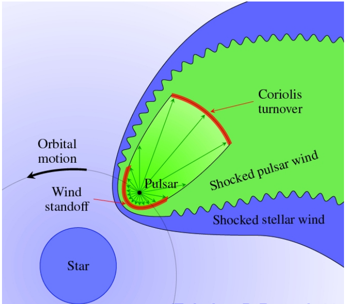

High-mass star+young psr (Zabalza, B-R, et al. 2013)

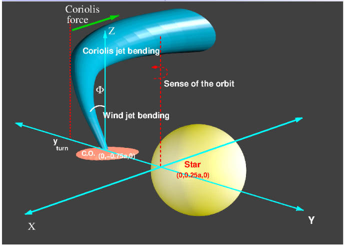

High-mass microquasar (B-R & Barkov 2016)

Non-accreting vs accreting HMGB

- **A non-accreting HMGB consists of a young pulsar plus an OB star whose winds interact in the ejector regime (mostly).**
- **A HMMQ consists of a CO plus an OB star in which the wind is accreted and jets form, which interact with the wind.**
- **In both cases, outflows interacting along the orbit are complex and emit radio, X- and γ-rays, likely through synchrotron and IC, plus $\gamma\gamma$...**

(e.g., B-R, Khangulyan, Aharonian, Barkov, Perucho + ...;

Bogovalov, + ...; Romero, + ...; Dubus, Lamberts, Cerutti + ...;

Sierpowska-Bartosik, Torres, Papitto + ...; Bednarek, + ...;

Huber, Kissmann, Reimer, + ...; Yoon, Heinz, Zdziarski + ...;

Chernyakova, Neronov, + ...; Takata, Kong, Cheng, + ...; etc.)

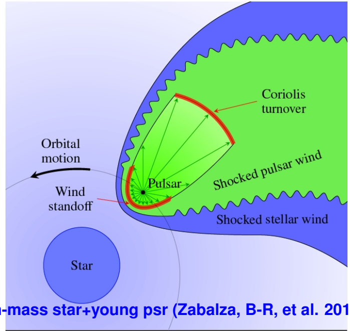

High-mass star+young psr (Zabalza, B-R, et al. 2013)

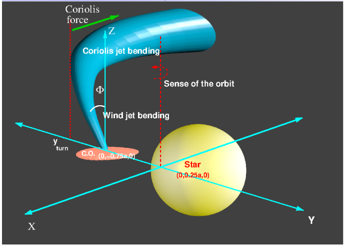

High-mass microquasar (B-R & Barkov 2016)

Non-accreting vs accreting HMGB

- **A non-accreting HMGB consists of a young pulsar plus an OB star whose winds interact in the ejector regime (mostly).**
- **A HMMQ consists of a CO plus an OB star in which the wind is accreted and jets form, which interact with the wind.**
- **In both cases, outflows interacting along the orbit are complex and emit radio, X- and γ-rays, likely through synchrotron and IC, plus $\gamma\gamma$...**

(e.g., B-R, Khangulyan, Aharonian, Barkov, Perucho + ...;

Bogovalov, + ...; Romero, + ...; Dubus, Lamberts, Cerutti + ...;

Sierpowska-Bartosik, Torres, Papitto + ...; Bednarek, + ...;

Huber, Kissmann, Reimer, + ...; Yoon, Heinz, Zdziarski + ...;

Chernyakova, Neronov, + ...; Takata, Kong, Cheng, + ...; etc.)

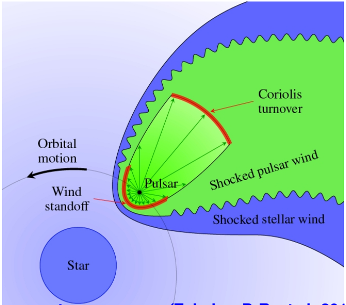

High-mass star+young psr (Zabalza, B-R, et al. 2013)

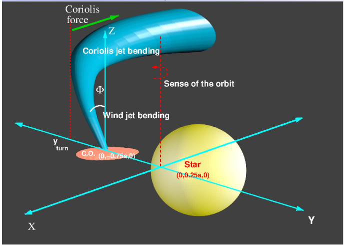

High-mass microquasar (B-R & Barkov 2016)

Non-accreting HMGB

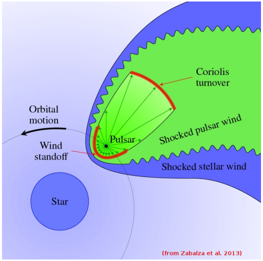

(Zabalza, B-R, et al. 2013)

RHD simulations with PLUTO of 2-wind-orbit interactions (low *e*).

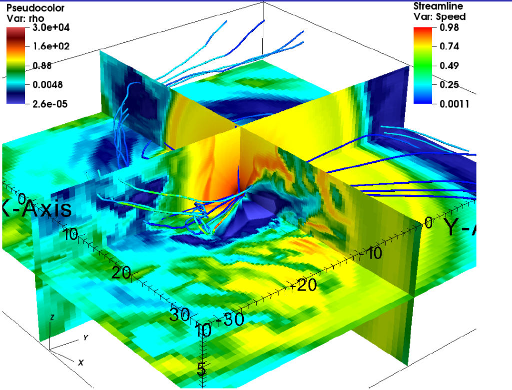

Fig. 2. Representation of the distribution of density in the XY-, XZ-, and YZ-planes for 3DIf at t = 3.9 days (apastron). Streamlines are shown in 3D.

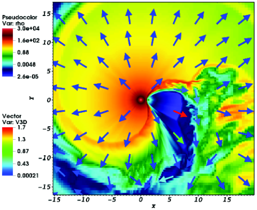

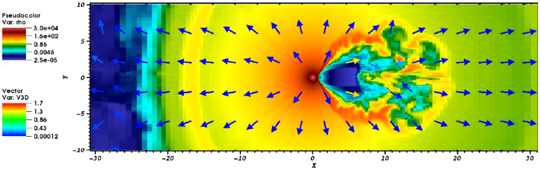

(LS 5039 at apastron; B-R, Barkov & Perucho 2015)

High-mass microquasar

RHD simulations with PLUTO of jet-wind-orbit interactions.

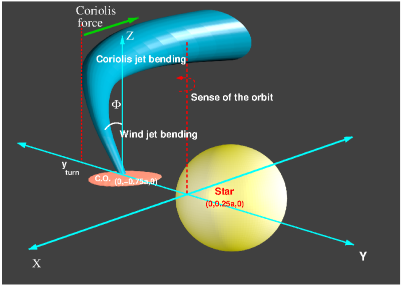

(HMMQ, $e = 0$; B-R & Barkov 2016; Barkov & B-R 2021)

Focus on non-accreting HMGB scenario, but those are qualitatively similar to HMMQ (not solving misteries here).

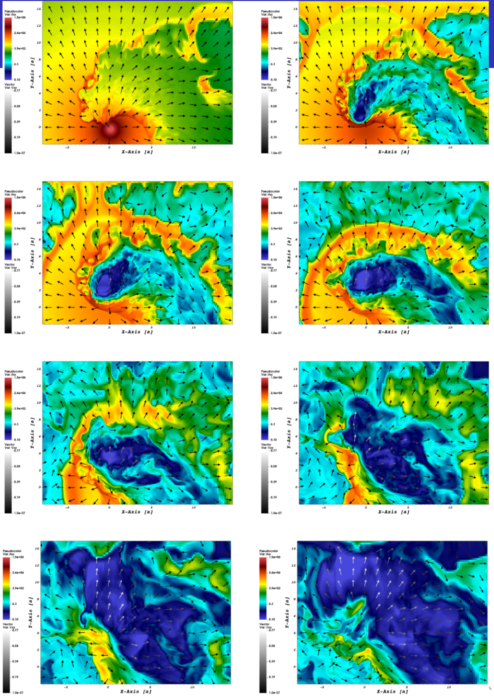

Outline

LS 5039 at high energies

- **O6.5V(f) + a possible neutron star at** $\approx$ **2 kpc**
- $P \approx 3.9$ **days and** $e \approx 0.35$
- **Reaching** $\approx 2 \times 10^{35}$ **(GeV) and** 5×10^{33} **erg s**$^{-1}$ **(TeV).**
- **MeV detection (consistent variability and SED) reaching** $\approx 5 \times 10^{35}$ **erg s**$^{-1}$**.**

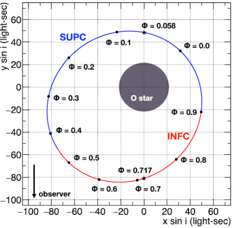

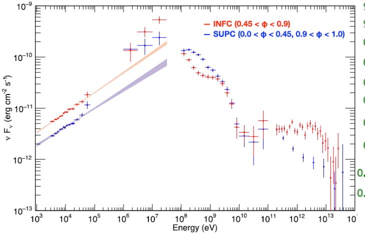

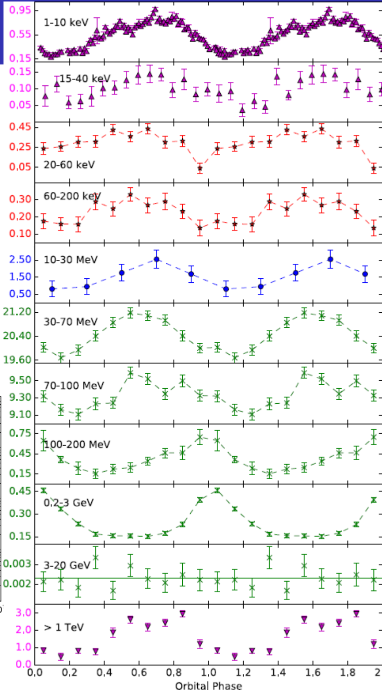

(Casares et al. 2005a; Aharonian et al. 2006; Takahashi et al. 2009; Chang et al. 2016; Yoneda et al. 2021)

LS 5039 $>$ 10 TeV

Moderately eccentric, compact, O+CO? binary

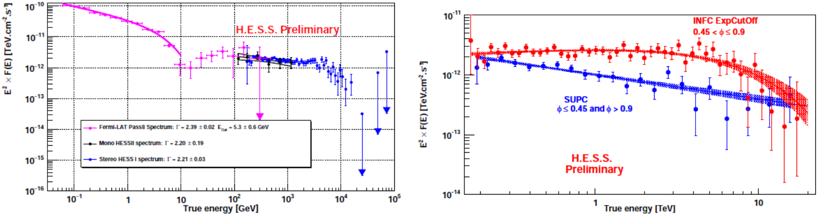

FIGURE 4. *Left*: SEDs obtained from monoscopic and a stereoscopic analyses of the H.E.S.S.-II and H.E.S.S.-I data sets, respectively. Results of fits with power-law functions are given in the inset. Also an SED obtained from a re-analysis of Fermi-LAT data is shown. *Right*: SEDs resulting from H.E.S.S.-I analyses for parts of the orbit corresponding to the inferior or superior conjunction. The corresponding orbital phase ranges are given for reference. Fit results are given in the main text.

Detected by HAWC up to $\sim$ 100 TeV.

(HESS: Bordas et al. 2015; Goodman, Gamma2022)

1FGL J1018.6−5856 at high energies

- **O6V(f) + a possible neutron star at ≈ 6.4 kpc**
- $P \approx 16.6$ **days and** $e \approx 0.53$
- **Reaching** $\approx 10^{36}$ **(HE) and** 5×10^{33} **erg** s^{-1} **(VHE)**
- **Possibly detected in MeV**

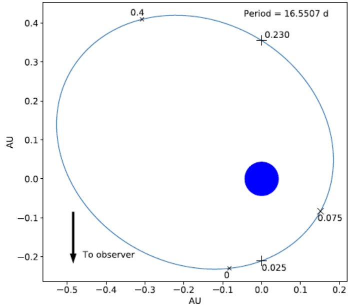

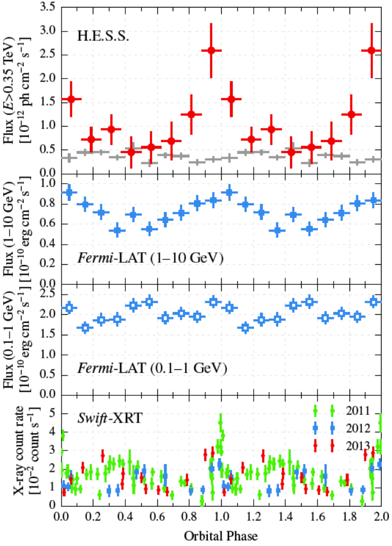

(Ackermann et al. 2012; HESS 2015; Collmar, VGGRS 2017; van Soelen et al. 2022)

1FGL J1018.6−5856 > 10 TeV

Moderately eccentric?, relatively compact, O+CO? binary (10s)

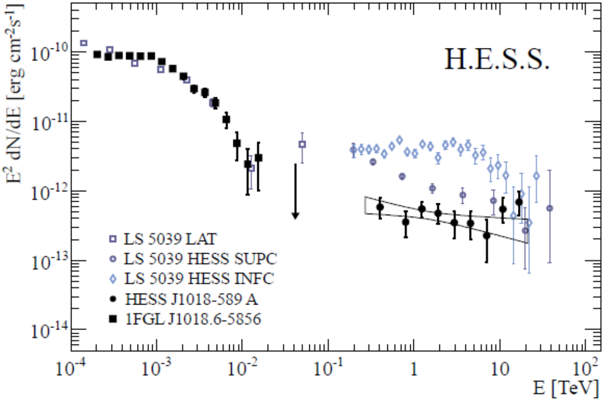

(HESS 2015)

Fig. 1. SED of HESS J1018–589 A/1FGL J1018.6–5856 is shown in black (filled squares and circles for the LAT and HESS detection). For comparison, the SEDs of LS 5039 during superior (SUPC) and inferior conjunction (INFC) are also included (blue points from Hadasch et al. 2012; Aharonian et al. 2005a).

LMC P3 at high energies

- **O5III(f)** $+$ **a possible neutron star at** $\approx$ 50 **kpc**
- $P \approx 10.3$ **days and** $e \approx 0.4$
- **Reaching** $\approx 4 \times 10^{36}$ **(HE) and** 5×10^{35} **erg** $\mathbf{s^{-1}}$ **(VHE)**

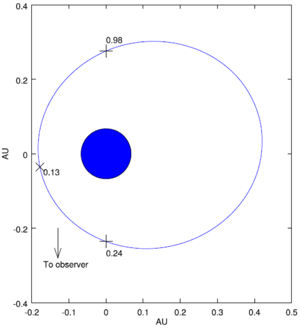

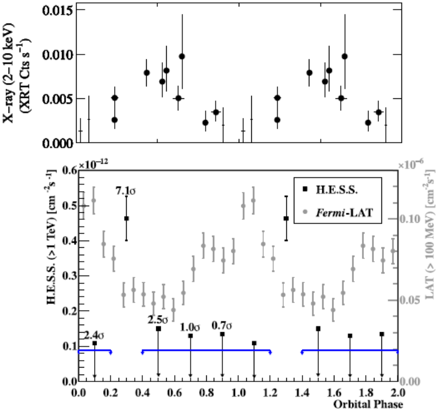

(Corbet et al. 2016; HESS 2018; van Soelen et al. 2019)

LMC P3 $>$ 10 TeV

Moderately eccentric, compact, O+CO? binary

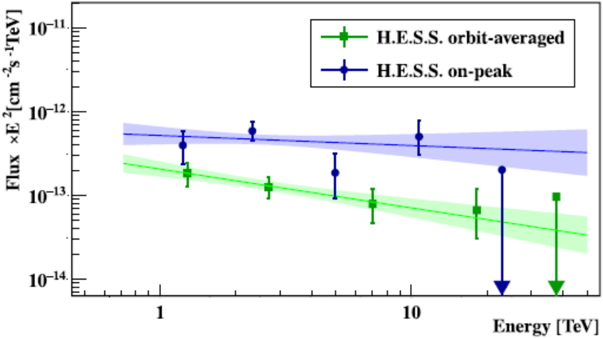

(HESS 2018)

Fig. 3. Spectral energy distribution averaged over the full orbit (green, squares) and for the on-peak orbital phase range (orbital phase from 0.2 to 0.4: blue, circles). The data points have 1 σ statistical error bars, upper limits are for a 95% confidence level. The best fit and its uncertainty are represented by the solid lines and shaded areas, respectively.

LS I +61 303 at high energies

- **B0V(e) + a likely neutron star at ≈ 2 kpc**
- $P \approx 26.5$ **days and** $e \approx 0.6 - 0.7$
- **Reaching** $\approx 2 \times 10^{35}$ **(HE) and** 5×10^{33} **erg** $\mathbf{s^{-1}}$ **(VHE)**
- **Similar MeV SED to LS 5039**

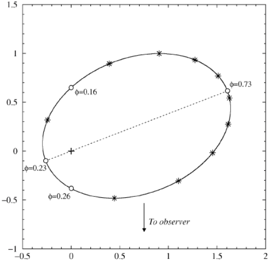

(Casares et al. 2005b; Albert et al. 2006; Zhang et al. 2010; Hadasch et al. 2012; Collmar, VGGRS 2017)

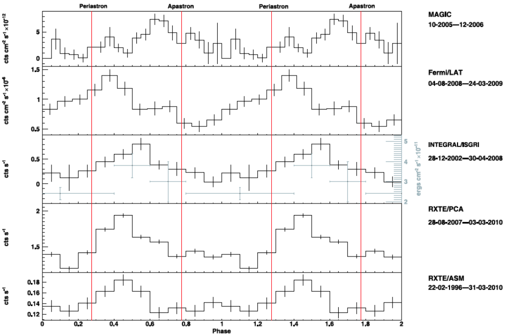

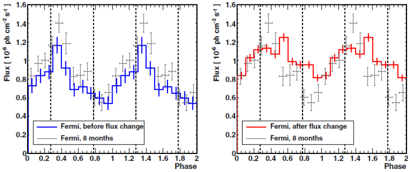

Messy behavior due to superorbital modulation.

Eccentric, relatively compact, Be+pulsar? binary

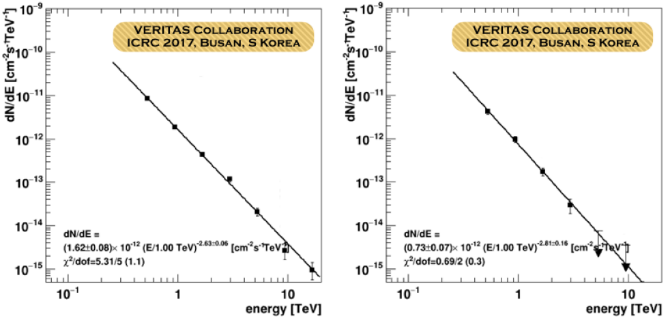

Figure 3: Spectral energy distribution (SED) for LS I +61°303 for two parts of the orbit (parts of the orbit shown on top panels). SED on the *left* is near apastron passage covering $\phi = 0.5 \rightarrow 0.8$ and SED on the *right* is for the rest of the orbit for $\phi = 0.8 \rightarrow 0.5$. The orbital parameters shown on top panel are used from [14]

(VERITAS: Kar et al. 2017)

Outline

Radiation modelling

- **Cooling: syn., IC, adiabatic**
- **$< MeV$ dominated by syn. (IC?), and GeV (syn.?) and TeV by IC.**
- **Important: γ-ray reprocessing.**

(e.g., Bednarek 1997; B-R & Khangulyan 2009; Takahashi+09)

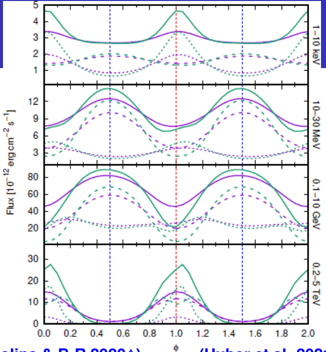

(e.g., ↓Molina & B-R 2020↑) **(Huber et al. 2021↓)**

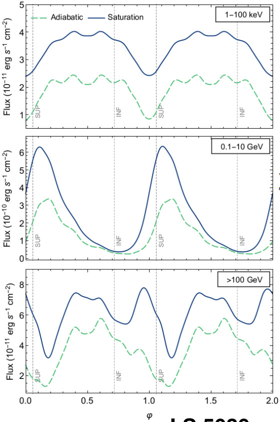

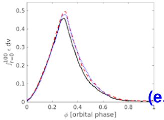

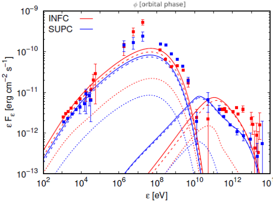

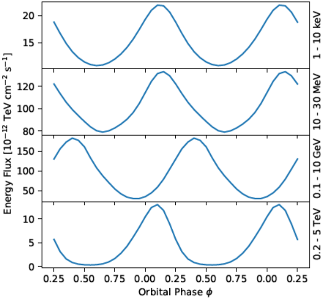

(e.g., Kefala & B-R) **LS 5039 and e effects**

$a = 0.2$ **AU**, $e = 0$, $\phi_{\rm inf,sup} = 0, 0.5$

Radiation modelling

- **Cooling: syn., IC, adiabatic**
- **$< MeV$ dominated by syn. (IC?), and GeV (syn.?) and TeV by IC.**
- **Important: γ-ray reprocessing.**

(e.g., Bednarek 1997; B-R & Khangulyan 2009; Takahashi+09)

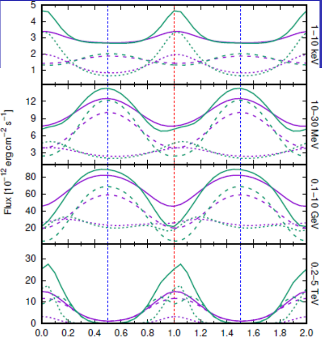

(e.g., ↓Molina & B-R 2020↑) **(Huber et al. 2021↓)**

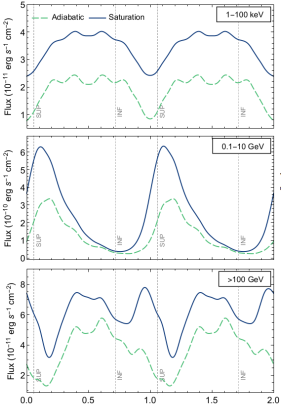

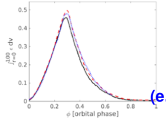

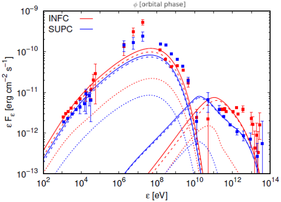

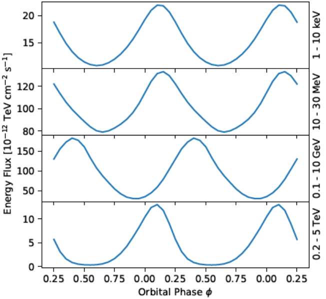

(e.g., Kefala & B-R) **LS 5039 and *e* effects**

$a = 0.2$ **AU**, $e = 0$, $\phi_{\rm inf,sup} = 0, 0.5$

Radiation modelling

- **Cooling: syn., IC, adiabatic**
- $<$ ***MeV*** **dominated by syn. (IC?), and GeV (syn.?) and TeV by IC.**
- **Important: γ-ray reprocessing.**

(e.g., Bednarek 1997; B-R & Khangulyan 2009; Takahashi+09)

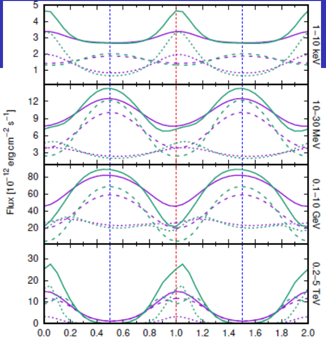

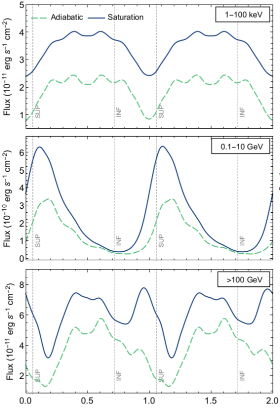

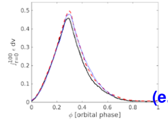

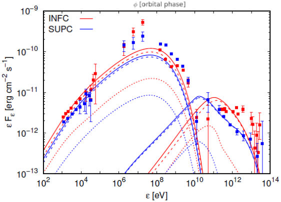

(e.g., ↓Molina & B-R 2020↑) **(Huber et al. 2021↓)**

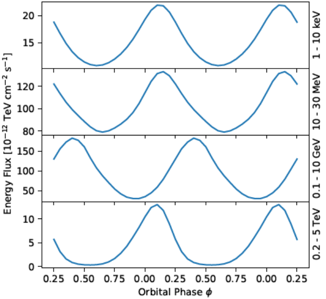

(e.g., Kefala & B-R) **LS 5039 and *e* effects** $a = 0.2$ **AU**, $e = 0$, $\phi_{\rm inf,sup} = 0, 0.5$

Phenomenological $E_{\max}$ in HMGB

- **Different acceleration sites, and mechanisms (Fermi I, II, shear; *B* reconnection; converter mechanism).**

  (e.g., Rieger et al. 2007; B-R 2012; B-R & Rieger 2012, Derishev & Aharonian 2012)

- **$E_{\max}$ for the most relevant processes ($t_{\rm acc} \sim \eta E/qBc$; $D \sim \chi D_{\rm Bohm}$; $RB \sim$ct?):**
  - **Hillas limit ($e^{\pm}$, p):**
    $E_{\max}^{\rm H} \sim 300\, R_{12}\, B_0$ TeV
  - **Escape/adiabatic loss ($e^{\pm}$, p):**
    $E_{\max}^{\rm dy} \sim 90\, R_{12}\, B_0\, v_{10}^{-1}\, \eta_1^{-1}$ TeV
  - **Diffusion ($e^{\pm}$, p):**
    $E_{\max}^{\rm diff} \sim 40\, R_{12}\, B_0\, \eta_1^{-1/2}\, \chi_1^{-1/2}$ TeV
  - **Synchrotron ($e^{\pm}$):**
    $E_{\max}^{\rm sy} \sim 20\, \eta_1^{-1/2}\, B_0^{-1/2}$ TeV

  (e.g., Khangulyan et al. 2008; B-R & Khangulyan 2009; Takahashi et al. 2009)

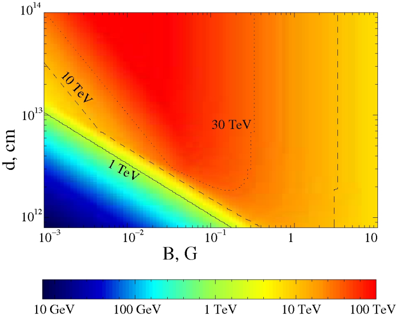

(↑ Khangulyan et al. 2008;↓ Bordas et al. 2015)

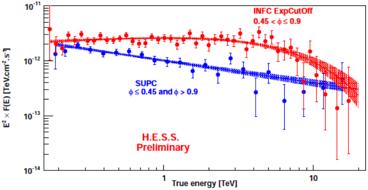

LS 5039: detected at $\sim$ 100 TeV by HAWC.

- **Different acceleration sites, and mechanisms (Fermi I, II, shear; *B* reconnection; converter mechanism).**
  (e.g., Rieger et al. 2007; B-R 2012; B-R & Rieger 2012, Derishev & Aharonian 2012)
- **$E_{\max}$ for the most relevant processes ($t_{\rm acc}\sim\eta E/qBc$; $D\sim\chi D_{\rm Bohm}$; $RB\sim$ct?):**
  - **Hillas limit ($e^{\pm}$, p):** $E_{\max}^{\rm H}\sim 300\,R_{12}\,B_0$ **TeV**
  - **Escape/adiabatic loss ($e^{\pm}$, p):** $E_{\max}^{\rm dy}\sim 90\,R_{12}\,B_0\,v_{10}^{-1}\,\eta_1^{-1}$ **TeV**
  - **Diffusion ($e^{\pm}$, p):** $E_{\max}^{\rm diff}\sim 40\,R_{12}\,B_0\,\eta_1^{-1/2}\,\chi_1^{-1/2}$ **TeV**
  - **Synchrotron ($e^{\pm}$):** $E_{\max}^{\rm sy}\sim 20\,\eta_1^{-1/2}\,B_0^{-1/2}$**TeV**

(e.g., Khangulyan et al. 2008; B-R & Khangulyan 2009; Takahashi et al. 2009)

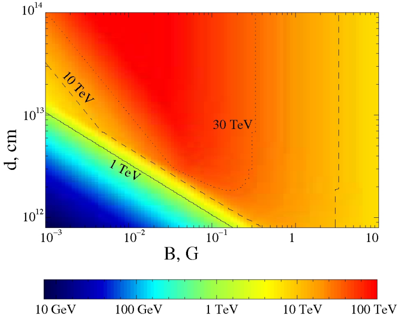

(↑ Khangulyan et al. 2008;↓ Bordas et al. 2015)

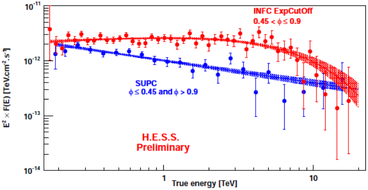

LS 5039: detected at $\sim$ 100 TeV by HAWC.

Phenomenological $E_{\max}$ in HMGB

- **Different acceleration sites, and mechanisms (Fermi I, II, shear; *B* reconnection; converter mechanism).**
  (e.g., Rieger et al. 2007; B-R 2012; B-R & Rieger 2012, Derishev & Aharonian 2012)
- **$E_{\max}$ for the most relevant processes ($t_{\rm acc} \sim \eta E/qBc$; $D \sim \chi D_{\rm Bohm}$; $RB \sim$ct?):**
  - **Hillas limit ($e^{\pm}$, p):** $E_{\max}^{\rm H} \sim 300\, R_{12}\, B_0$ **TeV**
  - **Escape/adiabatic loss ($e^{\pm}$, p):** $E_{\max}^{\rm dy} \sim 90\, R_{12}\, B_0\, v_{10}^{-1}\, \eta_1^{-1}$ **TeV**
  - **Diffusion ($e^{\pm}$, p):** $E_{\max}^{\rm diff} \sim 40\, R_{12}\, B_0\, \eta_1^{-1/2}\, \chi_1^{-1/2}$ **TeV**
  - **Synchrotron ($e^{\pm}$):** $E_{\max}^{\rm sy} \sim 20\, \eta_1^{-1/2}\, B_0^{-1/2}$**TeV**

(e.g., Khangulyan et al. 2008; B-R & Khangulyan 2009; Takahashi et al. 2009)

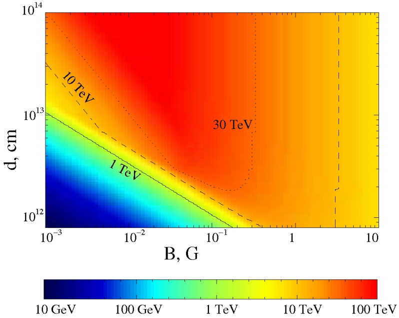

(↑ Khangulyan et al. 2008;↓ Bordas et al. 2015)

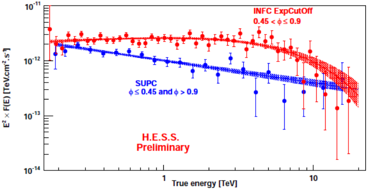

LS 5039: detected at $\sim$ 100 TeV by HAWC.

- **Different acceleration sites, and mechanisms (Fermi I, II, shear; B reconnection; converter mechanism).**
  (e.g., Rieger et al. 2007; B-R 2012; B-R & Rieger 2012, Derishev & Aharonian 2012)
- **$E_{\max}$ for the most relevant processes ($t_{\rm acc} \sim \eta E/qBc$; $D \sim \chi D_{\rm Bohm}$; $RB \sim$ct?):**
  - **Hillas limit ($e^{\pm}$, p):**
    $E^{\rm H}_{\max} \sim 300\, R_{12}\, B_0$ **TeV**
  - **Escape/adiabatic loss ($e^{\pm}$, p):**
    $E^{\rm dy}_{\max} \sim 90\, R_{12}\, B_0\, v_{10}^{-1}\, \eta_1^{-1}$ **TeV**
  - **Diffusion ($e^{\pm}$, p):**
    $E^{\rm diff}_{\max} \sim 40\, R_{12}\, B_0\, \eta_1^{-1/2}\, \chi_1^{-1/2}$ **TeV**
  - **Synchrotron ($e^{\pm}$):**
    $E^{\rm sy}_{\max} \sim 20\, \eta_1^{-1/2}\, B_0^{-1/2}$**TeV**

(e.g., Khangulyan et al. 2008; B-R & Khangulyan 2009; Takahashi et al. 2009)

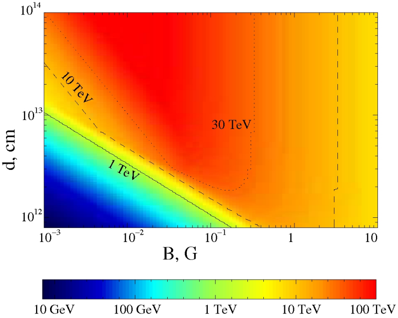

(↑ Khangulyan et al. 2008;↓ Bordas et al. 2015)

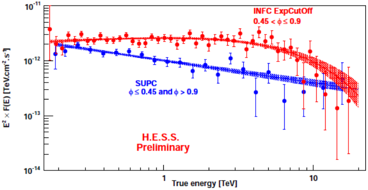

LS 5039: detected at ~ 100 TeV by HAWC.

Phenomenological $E_{\rm max}$ in HMGB

- **Different acceleration sites, and mechanisms (Fermi I, II, shear; B reconnection; converter mechanism).**
  (e.g., Rieger et al. 2007; B-R 2012; B-R & Rieger 2012, Derishev & Aharonian 2012)
- **$E_{\rm max}$ for the most relevant processes ($t_{\rm acc} \sim \eta E/qBc$; $D \sim \chi D_{\rm Bohm}$; $RB \sim$ct?):**
  - **Hillas limit ($e^\pm$, p):**
    $E_{\rm max}^{\rm H} \sim 300\, R_{12}\, B_0$ **TeV**
  - **Escape/adiabatic loss ($e^\pm$, p):**
    $E_{\rm max}^{\rm dy} \sim 90\, R_{12}\, B_0\, v_{10}^{-1}\, \eta_1^{-1}$ **TeV**
  - **Diffusion ($e^\pm$, p):**
    $E_{\rm max}^{\rm diff} \sim 40\, R_{12}\, B_0\, \eta_1^{-1/2}\, \chi_1^{-1/2}$ **TeV**
  - **Synchrotron ($e^\pm$):**
    $E_{\rm max}^{\rm sy} \sim 20\, \eta_1^{-1/2}\, B_0^{-1/2}$**TeV**

(e.g., Khangulyan et al. 2008; B-R & Khangulyan 2009; Takahashi et al. 2009)

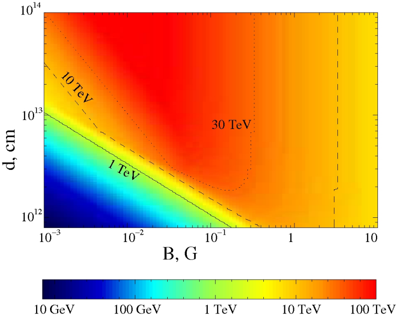

(↑ Khangulyan et al. 2008;↓ Bordas et al. 2015)

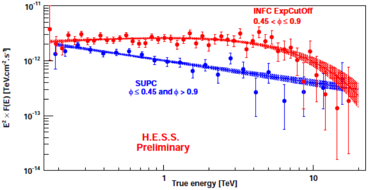

LS 5039: detected at ~ 100 TeV by HAWC.

Phenomenological $E_{\rm max}$ in HMGB

- **Different acceleration sites, and mechanisms (Fermi I, II, shear; *B* reconnection; converter mechanism).**

  (e.g., Rieger et al. 2007; B-R 2012; B-R & Rieger 2012, Derishev & Aharonian 2012)

- **$E_{\rm max}$ for the most relevant processes ($t_{\rm acc} \sim \eta E/qBc$; $D \sim \chi D_{\rm Bohm}$; $RB \sim$ct?):**
  - **Hillas limit ($e^{\pm}$, p):**
    $E^{\rm H}_{\rm max} \sim 300\, R_{12}\, B_0$ **TeV**
  - **Escape/adiabatic loss ($e^{\pm}$, p):**
    $E^{\rm dy}_{\rm max} \sim 90\, R_{12}\, B_0\, v_{10}^{-1}\, \eta_1^{-1}$ **TeV**
  - **Diffusion ($e^{\pm}$, p):**
    $E^{\rm diff}_{\rm max} \sim 40\, R_{12}\, B_0\, \eta_1^{-1/2}\, \chi_1^{-1/2}$ **TeV**
  - **Synchrotron ($e^{\pm}$):**
    $E^{\rm sy}_{\rm max} \sim 20\, \eta_1^{-1/2}\, B_0^{-1/2}$**TeV**

(e.g., Khangulyan et al. 2008; B-R & Khangulyan 2009; Takahashi et al. 2009)

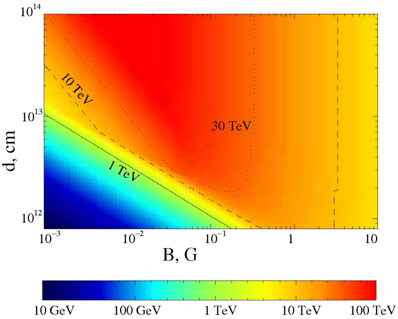

(↑ Khangulyan et al. 2008;↓ Bordas et al. 2015)

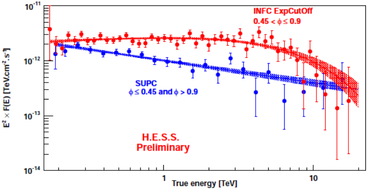

LS 5039: detected at ~ 100 TeV by HAWC.

Outline

The unshocked pulsar wind

- **The unshocked pulsar wind efficiently comptonizes star photons.**
  (e.g., Bogovalov & Aharonian 2000; Khangulyan et al. 2008; Cerutti et al. 2008; Sierpowska-Bartosik & Torres 2007; B-R 2021)
- **Derishev & Aharonian (2012) showed that the converter mechanism (Derishev et al. 2003; Stern 2003) can operate in compact HMGB via $e^{\pm}$-creation in the unshocked pulsar wind.**
- **The wind gets loaded and brakes while providing a Γ^2-boost to new $e^{\pm}$ that can reach $\gamma \sim 10^8$, which cool little in the unshocked wind.**
- **A 1–100 MeV component arises from postshock synchrotron.**
- **This mechanism can explain $t_{\rm acc} \sim E/qBc$, 1–100 MeV bumps, alleviate constraints from the unshocked wind, and heavily contribute to the global SED.**

(Derishev & B-R, in prep.)

The unshocked pulsar wind

- **The unshocked pulsar wind efficiently comptonizes star photons.** (e.g., Bogovalov & Aharonian 2000; Khangulyan et al. 2008; Cerutti et al. 2008; Sierpowska-Bartosik & Torres 2007; B-R 2021)
- **Derishev & Aharonian (2012) showed that the converter mechanism (Derishev et al. 2003; Stern 2003) can operate in compact HMGB via $e^{\pm}$-creation in the unshocked pulsar wind.**
- The wind gets loaded and brakes while providing a Γ^2-boost to new $e^{\pm}$ that can reach $\gamma \sim 10^8$, which cool little in the unshocked wind.
- A 1–100 MeV component arises from postshock synchrotron.
- This mechanism can explain $t_{\rm acc} \sim E/qBc$, 1–100 MeV bumps, alleviate constraints from the unshocked wind, and heavily contribute to the global SED.

(Derishev & B-R, in prep.)

The unshocked pulsar wind

- **The unshocked pulsar wind efficiently comptonizes star photons.**
  (e.g., Bogovalov & Aharonian 2000; Khangulyan et al. 2008; Cerutti et al. 2008; Sierpowska-Bartosik & Torres 2007; B-R 2021)
- **Derishev & Aharonian (2012) showed that the converter mechanism (Derishev et al. 2003; Stern 2003) can operate in compact HMGB via $e^{\pm}$-creation in the unshocked pulsar wind.**
- **The wind gets loaded and brakes while providing a Γ^2-boost to new $e^{\pm}$ that can reach $\gamma \sim 10^8$, which cool little in the unshocked wind.**
- **A 1–100 MeV component arises from postshock synchrotron.**
- **This mechanism can explain $t_{\rm acc} \sim E/qBc$, 1–100 MeV bumps, alleviate constraints from the unshocked wind, and heavily contribute to the global SED.**

(Derishev & B-R, in prep.)

The unshocked pulsar wind

- **The unshocked pulsar wind efficiently comptonizes star photons.**
  (e.g., Bogovalov & Aharonian 2000; Khangulyan et al. 2008; Cerutti et al. 2008; Sierpowska-Bartosik & Torres 2007; B-R 2021)
- **Derishev & Aharonian (2012) showed that the converter mechanism (Derishev et al. 2003; Stern 2003) can operate in compact HMGB via $e^{\pm}$-creation in the unshocked pulsar wind.**
- **The wind gets loaded and brakes while providing a Γ^2-boost to new $e^{\pm}$ that can reach $\gamma \sim 10^8$, which cool little in the unshocked wind.**
- **A 1–100 MeV component arises from postshock synchrotron.**
- **This mechanism can explain $t_{\rm acc} \sim E/qBc$, 1–100 MeV bumps, alleviate constraints from the unshocked wind, and heavily contribute to the global SED.**

(Derishev & B-R, in prep.)

The unshocked pulsar wind

- **The unshocked pulsar wind efficiently comptonizes star photons.**
  (e.g., Bogovalov & Aharonian 2000; Khangulyan et al. 2008; Cerutti et al. 2008; Sierpowska-Bartosik & Torres 2007; B-R 2021)
- **Derishev & Aharonian (2012) showed that the converter mechanism (Derishev et al. 2003; Stern 2003) can operate in compact HMGB via $e^{\pm}$-creation in the unshocked pulsar wind.**
- **The wind gets loaded and brakes while providing a Γ^2-boost to new $e^{\pm}$ that can reach $\gamma \sim 10^8$, which cool little in the unshocked wind.**
- **A 1–100 MeV component arises from postshock synchrotron.**
- **This mechanism can explain $t_{\rm acc} \sim E/qBc$, 1–100 MeV bumps, alleviate constraints from the unshocked wind, and heavily contribute to the global SED.**

(Derishev & B-R, in prep.)

The binary vicinity...

- **The shocked flow reaccelerates; instabilities and shear layers grow.**
- A strong Coriolis shock forms, followed by weaker shocks.
- Turbulence and wind mixing leads to spiral disruption.
- Missing: *B*, stellar clumps, wind anisotropies, radiation backreaction.

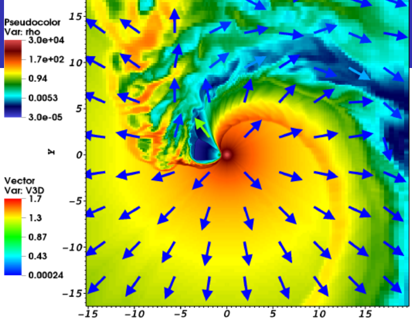

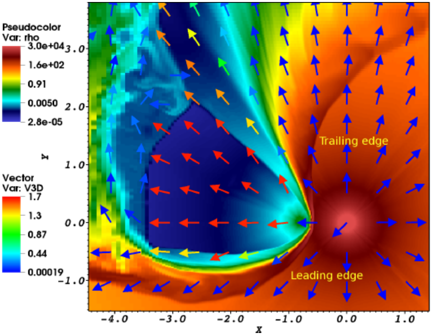

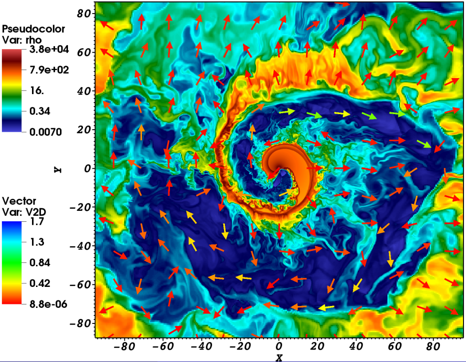

(B-R et al. 2012, 2015, for low *e*)

The binary vicinity...

- **The shocked flow reaccelerates; instabilities and shear layers grow.**
- **A strong Coriolis shock forms, followed by weaker shocks.**
- **Turbulence and wind mixing leads to spiral disruption.**
- **Missing: *B*, stellar clumps, wind anisotropies, radiation backreaction.**

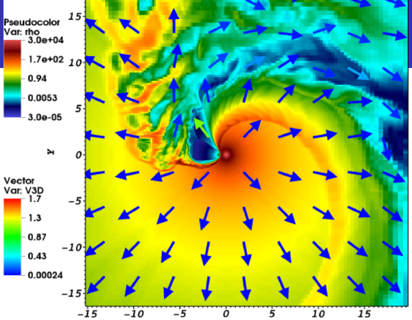

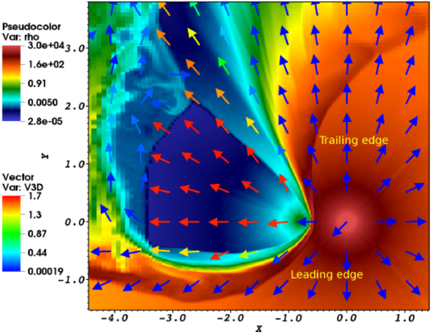

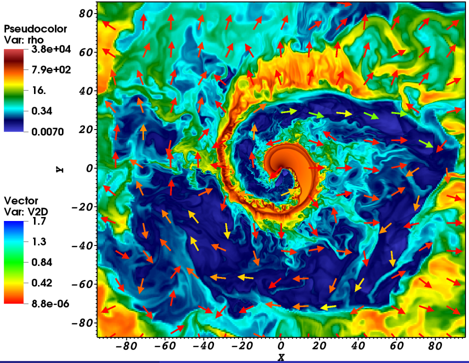

(B-R et al. 2012, 2015, for low *e*)

The binary vicinity...

- **The shocked flow reaccelerates; instabilities and shear layers grow.**
- **A strong Coriolis shock forms, followed by weaker shocks.**
- **Turbulence and wind mixing leads to spiral disruption.**
- **Missing: *B*, stellar clumps, wind anisotropies, radiation backreaction.**

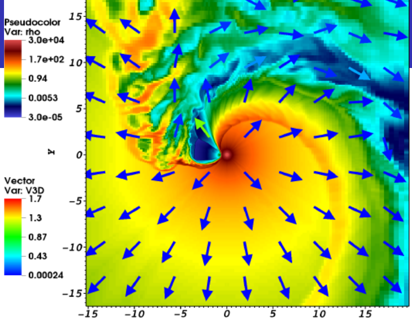

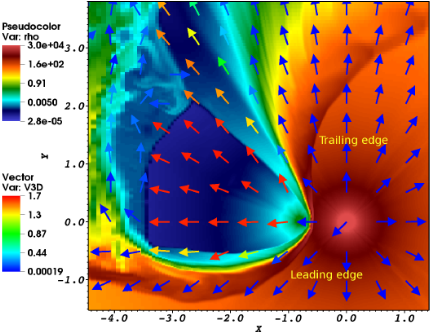

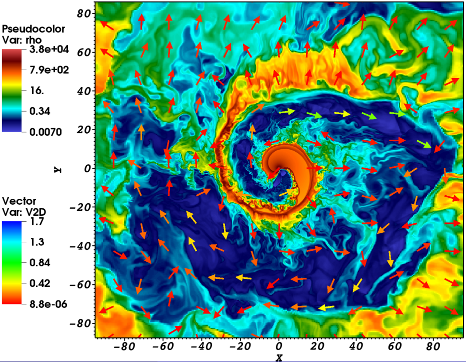

(B-R et al. 2012, 2015, for low *e*)

The binary vicinity...

- **The shocked flow reaccelerates; instabilities and shear layers grow.**
- **A strong Coriolis shock forms, followed by weaker shocks.**
- **Turbulence and wind mixing leads to spiral disruption.**
- **Missing: *B*, stellar clumps, wind anisotropies, radiation backreaction.**

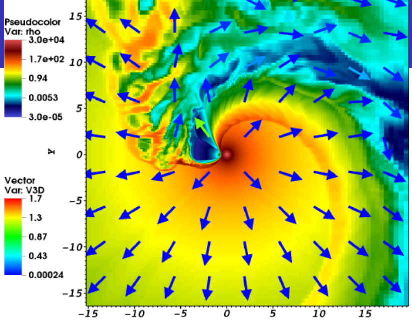

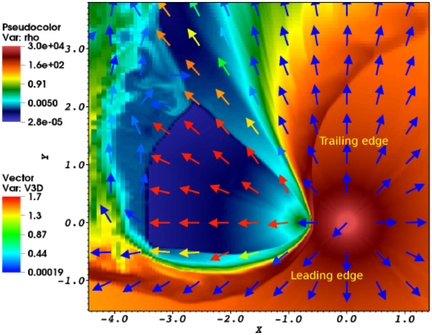

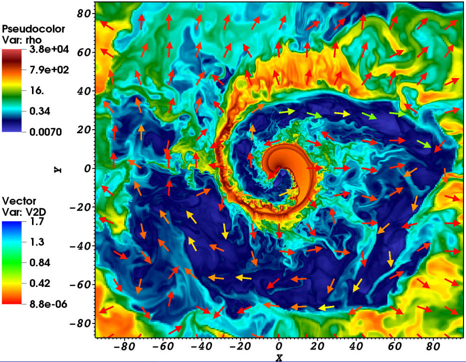

(B-R et al. 2012, 2015, for low *e*)

The binary vicinity...

- **The shocked flow reaccelerates; instabilities and shear layers grow.**
- **A strong Coriolis shock forms, followed by weaker shocks.**
- **Turbulence and wind mixing leads to spiral disruption.**
- **Missing: *B*, stellar clumps, wind anisotropies, radiation backreaction.**

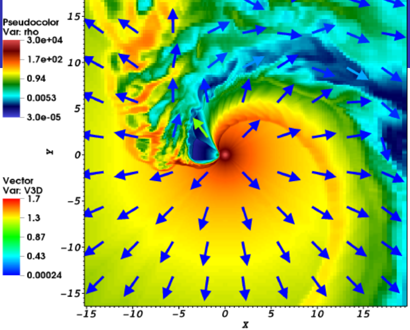

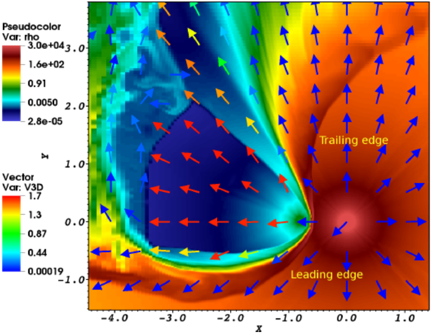

(B-R et al. 2012, 2015, for low *e*)

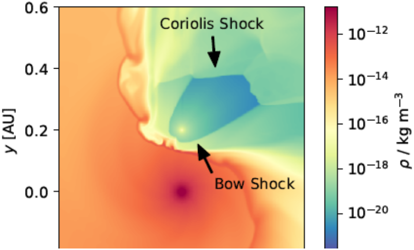

(see also Huber et al. 2021)

- **Coriolis shock region: optimal for acceleration and radiation.**
- Larger scales: energy dissipation softens, adiabatic losses dominate.
- Radio is a great tool to probe from the Coriolis shock outwards.
- Particles cool adiabatically before reaching the ISM.

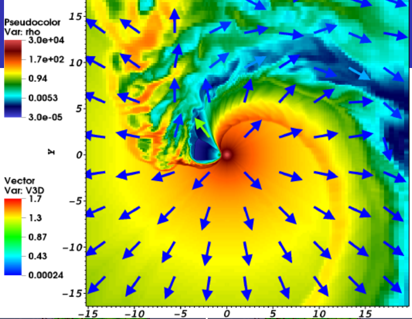

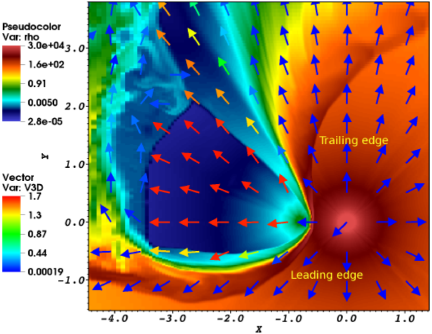

(B-R et al. 2012, 2015, for low *e*)

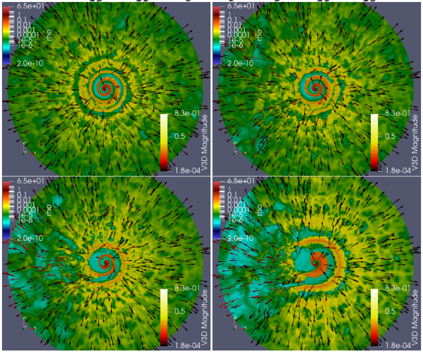

(see also Barkov & B-R 2021)

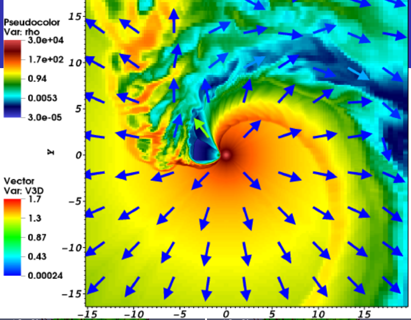

- **Coriolis shock region: optimal for acceleration and radiation.**
- **Larger scales: energy dissipation softens, adiabatic losses dominate.**
- **Radio is a great tool to probe from the Coriolis shock outwards.**
- **Particles cool adiabatically before reaching the ISM.**

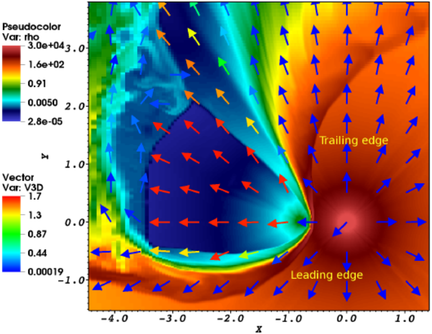

(B-R et al. 2012, 2015, for low *e*)

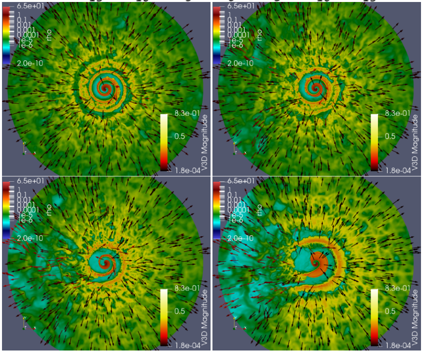

(see also Barkov & B-R 2021)

...and beyond

- **Coriolis shock region: optimal for acceleration and radiation.**
- **Larger scales: energy dissipation softens, adiabatic losses dominate.**
- **Radio is a great tool to probe from the Coriolis shock outwards.**
- **Particles cool adiabatically before reaching the ISM.**

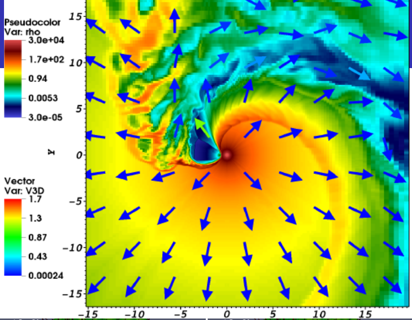

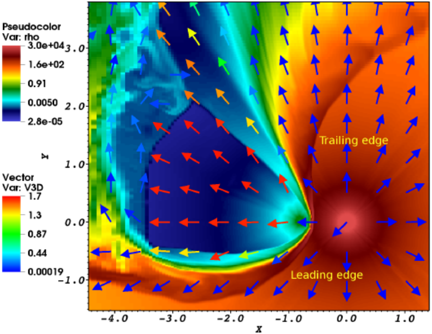

(B-R et al. 2012, 2015, for low *e*)

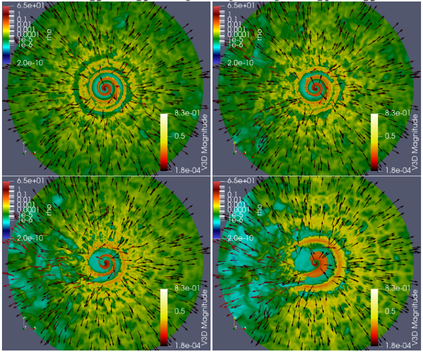

(see also Barkov & B-R 2021)

- Coriolis shock region: optimal for acceleration and radiation.
- Larger scales: energy dissipation softens, adiabatic losses dominate.
- Radio is a great tool to probe from the Coriolis shock outwards.
- Particles cool adiabatically before reaching the ISM.

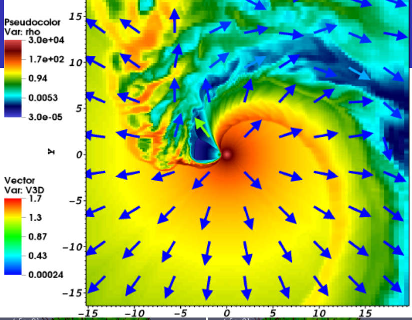

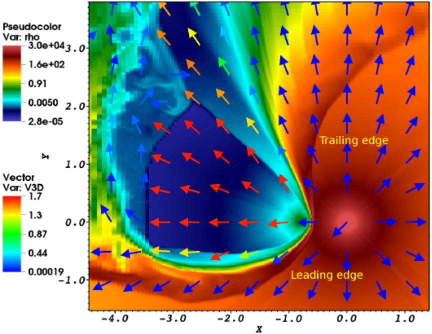

(B-R et al. 2012, 2015, for low *e*)

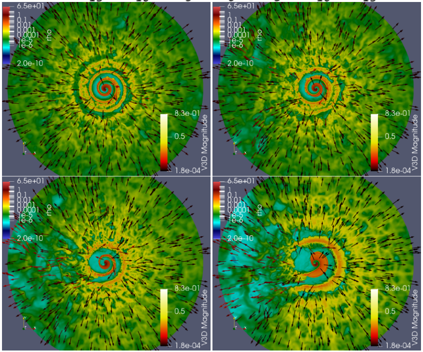

(see also Barkov & B-R 2021)

Eccentricity/The largest scales

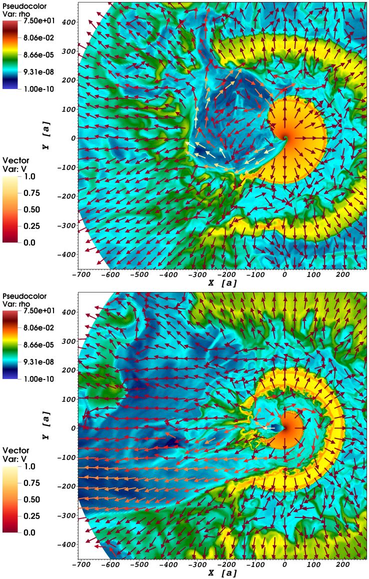

(Barkov & B-R 2018, for high e)

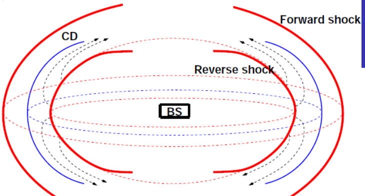

Flow termination. (B-R & Barkov 2011)

Mainly X-ray evidence.

(Paredes+2007 -LSI-; Durant+2011 -LS-; Pavlov+2015 -PSRB-, Williams+2015 -1FGL-; Kargaltsev+2021 -HESS-; Albacete-Colombo+2020 -PSRJ- ↓)

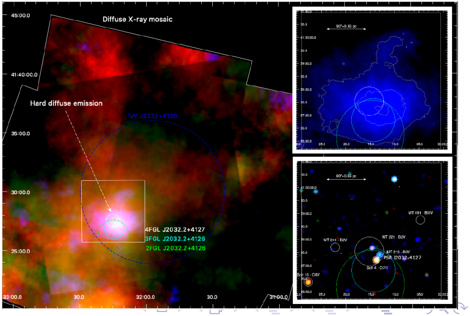

Outline

Final remarks

- **HMGB are perfect for multi-TeV particle acceleration and high-energy emission radiation.**
- **1st order factors: synchrotron and IC, radiation reprocessing, unshocked wind, eccentricity, Doppler boosting, and ED and MHD.**
- **Leptonic and hadronic CR injection from the system may be inefficient due to adiabatic losses.**
- **However, large-scale outflow-medium interactions might be suitable for PeV CR production, as suggested by large scale X-rays.**
- **Energetically, as several powerful HMGB are within $\sim 1/4$ of the disk, the total power of the population may be $\gtrsim 10^{38}$ erg $^{-1}$.**

Final remarks

- **HMGB are perfect for multi-TeV particle acceleration and high-energy emission radiation.**
- **1st order factors: synchrotron and IC, radiation reprocessing, unshocked wind, eccentricity, Doppler boosting, and ED and MHD.**
- **Leptonic and hadronic CR injection from the system may be inefficient due to adiabatic losses.**
- **However, large-scale outflow-medium interactions might be suitable for PeV CR production, as suggested by large scale X-rays.**
- **Energetically, as several powerful HMGB are within $\sim 1/4$ of the disk, the total power of the population may be $\gtrsim 10^{38}$ erg $^{-1}$.**

Final remarks

- **HMGB are perfect for multi-TeV particle acceleration and high-energy emission radiation.**
- **1st order factors: synchrotron and IC, radiation reprocessing, unshocked wind, eccentricity, Doppler boosting, and ED and MHD.**
- **Leptonic and hadronic CR injection from the system may be inefficient due to adiabatic losses.**
- **However, large-scale outflow-medium interactions might be suitable for PeV CR production, as suggested by large scale X-rays.**
- **Energetically, as several powerful HMGB are within $\sim 1/4$ of the disk, the total power of the population may be $\gtrsim 10^{38}$ erg $^{-1}$.**

Final remarks

- **HMGB are perfect for multi-TeV particle acceleration and high-energy emission radiation.**
- **1st order factors: synchrotron and IC, radiation reprocessing, unshocked wind, eccentricity, Doppler boosting, and ED and MHD.**
- **Leptonic and hadronic CR injection from the system may be inefficient due to adiabatic losses.**
- **However, large-scale outflow-medium interactions might be suitable for PeV CR production, as suggested by large scale X-rays.**
- **Energetically, as several powerful HMGB are within $\sim 1/4$ of the disk, the total power of the population may be $\gtrsim 10^{38}$ erg $^{-1}$.**

Final remarks

- **HMGB are perfect for multi-TeV particle acceleration and high-energy emission radiation.**
- **1st order factors: synchrotron and IC, radiation reprocessing, unshocked wind, eccentricity, Doppler boosting, and ED and MHD.**
- **Leptonic and hadronic CR injection from the system may be inefficient due to adiabatic losses.**
- **However, large-scale outflow-medium interactions might be suitable for PeV CR production, as suggested by large scale X-rays.**
- **Energetically, as several powerful HMGB are within $\sim 1/4$ of the disk, the total power of the population may be $\gtrsim 10^{38}$ erg $^{-1}$.**